Acta Crystallographica Section F
Structural Biology and Crystallization Communications
ISSN 1744-3091

Crystallographic characterization of the radixin FERM domain bound to the cytoplasmic tails of adhesion molecules CD43 and PSGL-1

Yumiko Takai,[a] Ken Kitano,[a] Shin-ichi Terawaki,[a] Ryoko Maesaki[a] and Toshio Hakoshima[a,b]*

[a]Structural Biology Laboratory, Nara Institute of Science and Technology, Keihanna Science City, Nara 630-0192, Japan, and [b]CREST, Japan Science and Technology Agency, Keihanna Science City, Nara 630-0192, Japan

Correspondence e-mail: hakosima@bs.naist.jp

Received 19 October 2006
Accepted 13 December 2006

Radixin is a member of the ERM proteins that cross-link plasma membranes and actin filaments. The FERM domains located in the N-terminal regions of ERM proteins are responsible for membrane association through direct interaction with the cytoplasmic tails of integral membrane proteins. Here, crystals of the radixin FERM domain bound to the cytoplasmic peptides of two adhesion molecules, CD43 and PSGL-1, have been obtained. Crystals of the radixin FERM domain bound to CD43 belong to space group $P4_322$, with unit-cell parameters $a = b = 68.72$, $c = 201.39$ Å, and contain one complex in the crystallographic asymmetric unit. Crystals of the radixin FERM domain bound to PSGL-1 belong to space group $P2_12_12_1$, with unit-cell parameters $a = 80.74$, $b = 85.73$, $c = 117.75$ Å, and contain two complexes in the crystallographic asymmetric unit. Intensity data sets were collected to a resolution of 2.9 Å for the FERM–CD43 complex and 2.8 Å for the FERM–PSGL-1 complex.

1. Introduction

Ezrin, radixin and moesin form the ERM family of proteins that link membrane proteins to the cytoskeleton and perform structural and regulatory roles at the polarized cell cortex (Bretscher, 1999; Mangeat *et al.*, 1999; Tsukita & Yonemura, 1999). ERM proteins consist of three functional domains: an N-terminal FERM (4.1, ezrin, radixin, moesin) domain, an extended coiled-coil region and a short C-terminal domain that binds F-actin. ERM proteins utilize the FERM domain to bind intracellular proteins such as ERM-binding phosphoprotein 50 (EBP50) and Rho GDP dissociation inhibitor (Reczek *et al.*, 1997; Takahashi *et al.*, 1997). The FERM domain associated with the plasmamembrane binds the juxtamembrane region of the cytoplasmic tails of transmembrane proteins such as intercellular adhesion molecules ICAM-1, ICAM-2 and ICAM-3 of the immunoglobulin superfamily, cell-surface hyaluronate receptor CD44, cell-surface glycoprotein CD43 (leukosialin or sialophorin), P-selectin glycoprotein ligand-1 (PSGL-1) and the abundant microvillar neutral endopeptidase 24.11 (NEP; Helander *et al.*, 1996; Yonemura *et al.*, 1993, 1998; Tsukita *et al.*, 1994; Alonso-Lebrero *et al.*, 2000; Iwase *et al.*, 2004). The adhesion molecules CD43 and PSGL-1 are expressed on leukocytes and belong to a family comprising mucin-type molecules. CD43, the major cell-surface molecule in most haematopoietic cells, is thought to possess both cell-adhesion and activation properties (Walker & Green, 1999). PSGL-1, which is expressed as a homodimer, mediates leukocyte adhesion to endothelial cells and is critically involved in the inflammatory response in both brain and peripheral tissues (McEver & Cummings, 1997). The cytoplasmic domain regions of PSGL-1 and CD43 have been shown to interact with the cytoskeleton during leukocyte emigration or activation and these interactions are thought to be mediated through the FERM domain of ERM proteins. A recent report detailing the crystal structure of the radixin FERM domain bound to ICAM-2 suggested that ICAM-2 and related adhesion molecules possess the Motif-1 sequence motif R*XX*TY*X*V*XX*A (where *X* represents any amino acid) for binding to the FERM domain (Hamada *et al.*, 2003). This sequence motif is less conserved in CD43 and PGSL-1. Moreover, the cytoplasmic domain regions of

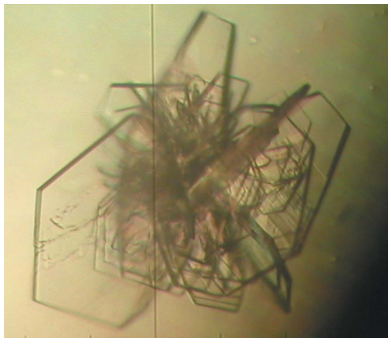

Table 1
X-ray diffraction data of the FERM–CD43 and FERM–PSGL-1 complex crystals.

Values in parentheses are for the outer resolution shell.

Complex	FERM–CD43	FERM–PSGL-1
Beamline (SPring-8)	BL44XU	BL41XU
Detector	DIP2040b IP	MAR CCD
Wavelength (Å)	0.90	1.00
Temperature (K)	100	100
Oscillation range (°)	180 (3° × 60 images)	180 (1° × 180 images)
Exposure time (s)	30	7
Space group	$P4_322$	$P2_12_12_1$
Unit-cell parameters (Å)	a = 68.72, b = 68.72, c = 201.39	a = 80.74, b = 85.73, c = 117.75
Resolution (Å)	2.9	2.8
Reflections (total/unique)	90704/11007	191709/20429
Completeness (%)	96.5 (76.4)	98.4 (92.3)
Mosaicity	0.6–1.0	0.6–1.5
$\langle I/\sigma(I)\rangle$	7.7 (1.7)	9.2 (3.7)
$R_{\rm merge}$† (%)	12.1 (37.7)	7.1 (11.7)

† $R_{\rm merge} = \sum|I_i - \langle I_i\rangle|/\sum\langle I_i\rangle$, where I_i is the observed intensity and $\langle I_i\rangle$ is the average intensity over symmetry-equivalent measurements.

these two adhesion molecules exhibit no homology to Motif-2, unlike the case with NHERF, where this sequence motif is utilized for binding to the FERM domain (Terawaki *et al.*, 2006). Here, we report the crystallization and preliminary crystallographic investigation of the radixin FERM domain complexed with the cytoplasmic domain regions of PSGL-1 (FERM–PSGL-1 complex) and CD43 (FERM–CD43 complex).

2. Methods

2.1. Protein preparation and binding assay

The FERM domain (residues 1–310, 36.7 kDa) of mouse radixin was expressed in BL21(DE3) RIL cells containing plasmid pGEX4T-3 as a fusion protein with glutathione-*S*-transferase. Details of this purification scheme have been described previously (Hamada *et al.*, 2000). The purified protein was verified using matrix-assisted laser desorption/ionization time-of-flight mass spectroscopy (MALDI–TOF MS; PerSeptive Inc.) and N-terminal analysis (M492; Applied Biosystems). Peptides corresponding to the cytoplasmic domain region of mouse CD43 and PSGL-1 were purchased from Toray Research Center (Tokyo, Japan). The peptide regions for binding assays and crystallization were determined according to previous studies of CD43 (Yonemura *et al.*, 1998) and PSGL-1 (Urzainqui *et al.*, 2002). Binding assays of these peptides to the FERM domain were performed by surface plasmon resonance measurements using a BIAcore Biosensor instrument (Biacore 3000, Biacore). Biotinylated peptides were immobilized on the surface of an SA sensor chip (sensor chip SA, Biacore). Purified FERM domain was injected onto the peptide surfaces. Kinetic parameters were evaluated using the *BIA* evaluation software (Biacore).

2.2. Crystallization

Crystallization was performed by the hanging-drop vapour-diffusion method using commercially available crystal screens at 277 K. Crystallization solutions were prepared by mixing 1 µl protein solution with 1 µl of each reservoir solution. The ratio of the FERM domain and peptide was adjusted from 1:1 to 1:20 in an effort to improve the crystallization conditions. Crystals of the FERM–CD43 complex were obtained using a 1:5 protein:peptide solution prepared by mixing a purified 1 m*M* radixin FERM-domain solution with 5 m*M* CD43 peptide (20 residues) solution in a 1:1 volume ratio (1:5 protein:peptide molar ratio). In the case of the FERM–PSGL-1 complex, use of a 1:10 protein:peptide solution was successful and was prepared by mixing a purified 1 m*M* radixin FERM-domain solution with 10 m*M* PSGL-1 peptide (18 residues) in a 1:1 volume ratio. The crystals obtained were transferred stepwise into a cryoprotective solution and flash-frozen at 100 K. MALDI–TOF MS was employed to confirm that crystals contained both the radixin FERM domain and the PSGL-1 or CD43 peptide.

2.3. X-ray data collection

X-ray diffraction data for the radixin FERM–CD43 crystal were collected using a DIP2040b image-plate detector installed on the BL44XU beamline at SPring-8, while X-ray diffraction data for the radixin FERM–PSGL-1 crystal were collected using an MAR CCD detector installed on the BL41XU beamline at SPring-8. All data were processed with the *HKL*-2000 program suite (Otwinowski & Minor, 1997).

3. Results and discussion

A quantitative analysis of peptide binding to the radixin FERM domain was performed. The CD43 peptide, which consists of 20 N-terminal residues from the cytoplasmic tail (272-RQRQKRRT-GALTLSGGGKRN-291) encompassing the reported binding region (Yonemura *et al.*, 1998), binds the radixin FERM domain with a dissociation constant ($K_{\rm d}$) of 1.96 µ*M* (data not shown). This binding affinity is comparable to that of the full-length cytoplasmic domain region. The PSGL-1 peptide of the juxtamembrane region, which consists of 18 N-terminal residues from the PSGL-1 cytoplasmic tail (331-RLSRKTHMYPVRNYSPTE-348; Urzainqui *et al.*, 2002), binds to the radixin FERM domain with a $K_{\rm d}$ of 201 n*M* and was not significantly different in comparison with the binding affinity of a longer PSGL-1 peptide comprising 32 residues ($K_{\rm d}$ = 350 n*M*).

Needle-like crystals of the FERM–CD43 complex were obtained within 5 d from a solution containing 1 µl of the 1:5 protein:peptide solution with 1 µl reservoir solution containing 100 m*M* sodium citrate pH 5.6, 10% polyethylene glycol 4000 (PEG 4K) and 10%(*v*/*v*) 2-propanol (Fig. 1). The crystals were transferred stepwise into a cryoprotective solution containing 11% PEG 4K, 18%(*v*/*v*) 2-propanol, 15% PEG 200 and 100 m*M* sodium citrate buffer and flash-frozen at 100 K. The FERM–CD43 crystals belong to space group $P4_322$ (or $P4_122$), with unit-cell parameters $a = b = 68.72$, $c = 201.39$ Å. MALDI–TOF MS of dissolved crystals gave peaks at

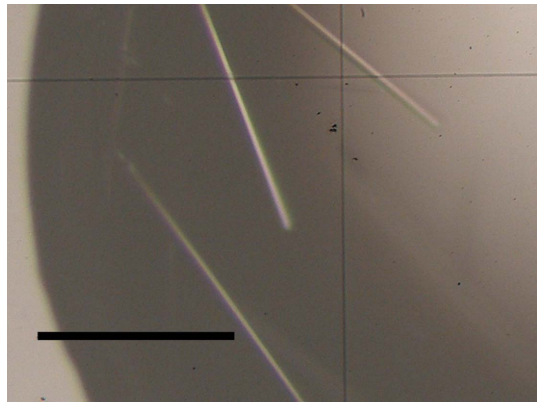

Figure 1
Crystals of the complex formed by the radixin FERM domain with the CD43 cytoplasmic tail peptide. The scale bar indicates 0.1 mm.

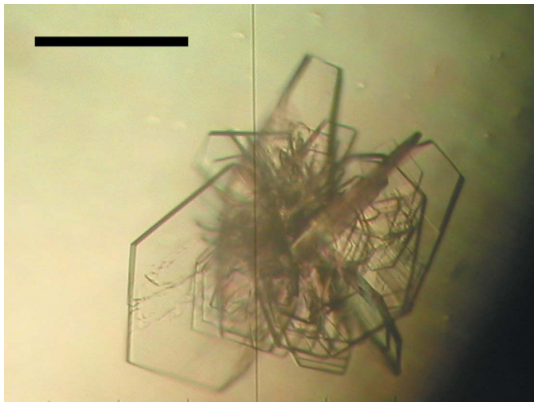

Figure 2
Crystals of the complex formed by the radixin FERM domain with the PSGL-1 cytoplasmic tail peptide. The scale bar indicates 0.2 mm.

37 921.3 Da (the calculated weight of the radixin FERM domain was 37 919 Da) and 2240.6 Da (the calculated weight of the CD43 peptide was 2240.5 Da), respectively, showing that the crystals contain both the protein and the peptide. A Matthews coefficient (Matthews, 1968) of 3.0 Å^3 Da^{-1} was calculated assuming the presence of one 1:1 radixin FERM domain–CD43 peptide complex in the asymmetric unit, which corresponds to 58.1% solvent content by volume. The crystallographic data and intensity data-processing statistics are summarized in Table 1.

Plate-like crystals of the FERM–PSGL-1 complex were obtained in a few days by mixing 1 µl 1:10 protein:peptide solution with 1 µl reservoir solution containing 100 m*M* Tris–HCl pH 8.2 and 8% polyethylene glycol 8000 (PEG 8K; Fig. 2). The crystals were transferred stepwise into a cryoprotective solution containing 8% PEG 8K, 100 m*M* Tris buffer and 20% PEG 400 and flash-frozen at 100 K. The FERM–PSGL-1 crystals belong to space group $P2_12_12_1$, with unit-cell parameters a = 80.74, b = 85.73, c = 117.75 Å. MALDI–TOF MS of dissolved crystals gave peaks at 37 920.7 Da (the calculated weight of the radixin FERM domain was 37 919 Da) and 2460.4 Da (the calculated weight of the PSGL-1 peptide was 2461.8 Da), respectively, showing that the crystals contain both the protein and the peptide. Assuming the presence of two 1:1 FERM–PSGL-1 complexes in the asymmetric unit, a Matthews coefficient of 2.5 Å^3 Da^{-1} was obtained, which corresponds to 50.9% solvent content by volume. Calculation of the self-rotation map did not yield a peak in the $\kappa = 180^\circ$ section, which suggests that the dimer is not associated with a local twofold symmetry or is associated with a noncrystallographic twofold axis that is parallel to the crystallographic 2_1 axis. Efforts are currently being directed towards solving both structure complexes using the molecular-replacement method.

We would like to thank J. Tsukamoto for technical support in performing the MALDI–TOF MS analysis and S. Sakurai for calculation of the rotation function. We gratefully acknowledge Sachiko Tsukita and Shoichiro Tsukita for providing mouse radixin cDNA. This work was supported in part by a Protein 3000 project on Signal Transduction from the Ministry of Education, Culture, Sports, Science and Technology (MEXT) of Japan (to TH). ST was supported by a Center of Excellence (COE) postdoctoral research fellowship of a Grant-in-Aid for the 21st Century COE Research from MEXT. RM was supported by a postdoctoral research fellowship for Young Scientists from the Japan Society for the Promotion of Science. We also acknowledge Drs N. Shimizu, M. Kawamoto and M. Yamamoto at SPring-8 for help during data collection at the synchrotron beamline BL41XU and Drs T. Tsukihara, A. Nakagawa, E. Yamashita and M. Yoshimura at SPring-8 for the use of synchrotron beamline BL44XU.

References

Alonso-Lebrero, J. L., Serrador, J. M., Domínguez-Jiménez, C., Barreiro, O., Luque, A., del Pozo, M. A., Snapp, K., Kansas, G., Schwartz-Albiez, R., Furthmayr, H., Lozano, F. & Sánchez-Madrid, F. (2000). *Blood*, **95**, 2413–2419.
Bretscher, A. (1999). *Curr. Opin. Cell Biol.* **11**, 109–116.
Hamada, K., Shimizu, T., Matsui, T., Tsukita, S., Tsukita, S. & Hakoshima, T. (2000). *EMBO J.* **19**, 4449–4462.
Hamada, K., Shimizu, T., Yonemura, S., Tsukita, S., Tsukita, S. & Hakoshima, T. (2003). *EMBO J.* **22**, 502–514.
Helander, T. S., Carpén, O., Turunen, O., Kovanen, P. E., Vaheri, A. & Timonen, T. (1996). *Nature (London)*, **382**, 265–268.
Iwase, A., Shen, R., Navarro, D. & Nanus, D. M. (2004). *J. Biol. Chem.* **279**, 11898–11905.
McEver, R. P. & Cummings, R. D. (1997). *J. Clin. Invest.* **100**, 485–491.
Mangeat, P., Roy, C. & Martin, M. (1999). *Trends Cell Biol.* **9**, 187–192.
Matthews, B. W. (1968). *J. Mol. Biol.* **33**, 491–497.
Otwinowski, Z. & Minor, W. (1997). *Methods Enzymol.* **276**, 307–326.
Reczek, D., Berryman, M. & Bretscher, A. (1997). *J. Cell Biol.* **139**, 169–179.
Takahashi, K., Sasaki, T., Mammoto, A., Takaishi, K., Kameyama, T., Tsukita, S., Tsukita, S. & Takai, Y. (1997). *J. Biol. Chem.* **272**, 23371–23375.
Terawaki, S., Maesaki, R. & Hakoshima, T. (2006). *Structure*, **14**, 777–789.
Tsukita, S., Oishi, K., Sato, N., Sagara, J., Kawai, A. & Tsukita, S. (1994). *J. Cell Biol.* **126**, 391–401.
Tsukita, S. & Yonemura, S. (1999). *J. Biol. Chem.* **274**, 34507–34510.
Urzainqui, A., Serrador, J. M., Viedma, F., Yáñez-Mó, M., Rodríguez, A., Corbí, A. L., Alonso-Lebrero, J. L., Luque, A., Deckert, M., Vázquez, J. & Sánchez-Madrid, F. (2002). *Immunity*, **17**, 401–412.
Walker, J. & Green, J. M. (1999). *J. Immunol.* **162**, 4109–4114.
Yonemura, S., Hirao, M., Doi, Y., Takahashi, N., Kondo, T., Tsukita, S. & Tsukita, S. (1998). *J. Cell Biol.* **140**, 885–895.
Yonemura, S., Nagafuchi, A., Sato, N. & Tsukita, S. (1993). *J. Cell Biol.* **120**, 437–449.